

Polyethylene Glycol Protects Injured Neuronal Mitochondria

Haiping Chen^a Eamon Quick^b Gary Leung^a Kristin Hamann^a Yan Fu^b
Ji-Xin Cheng^b Riyi Shi^{a, b}

^aDepartment of Basic Medical Sciences, Center for Paralysis Research and ^bWeldon School of Biomedical Engineering, Purdue University, West Lafayette, Ind., USA

Key Words

Reactive oxygen species · Surfactant · Membrane disruption · Mitochondrial respiration · Neuron · CARS

Abstract

Objective: Polyethylene glycol (PEG), a hydrophilic polymer, can immediately repair neuronal membranes and inhibit free radical production following trauma. The aim of this study is to examine whether PEG can directly repair mitochondria in the event of trauma. **Method:** Purified brain mitochondria from guinea pigs were used. Mitochondrial function was assessed by biochemical methods and structural changes were observed by both fluorescence light microscopy and coherent anti-Stokes Raman scattering microscopy. **Results:** We present evidence suggesting that PEG is capable of directly reducing injury to mitochondria independent of plasma membrane repair. Specifically, the suppression of oxygen consumption rate of purified mitochondria due to H₂O₂ and/or calcium can be significantly reversed by 12.5 mM PEG. PEG also significantly reduced mitochondrial swelling due to similar injury. Furthermore, we have shown that such PEG-mediated mitochondrial protection is dependent on the molecular weight of PEG, suggesting a direct physical blockade of mitochondrial permeability transitional pore by PEG. **Conclusion:** These findings, coupled with previous evidence that PEG enters the cytosol following mechanical trauma, strongly indicate that there are at least

2 avenues of PEG-mediated cytoprotection in mechanically injured spinal cords: repair of plasma membrane and protection of mitochondria.

Copyright © 2009 S. Karger AG, Basel

Introduction

It is well established that mechanical insults to the central nervous system, such as spinal cord injury and traumatic brain injury, inflict an immediate, primary injury characterized mainly by membrane disruption [1–6], as well as consequent oxidative stress, a hallmark of secondary injury [7–11]. The combination of primary and secondary injury contributes to the profound functional loss and structural damage seen in such injuries [12, 13]. We have previously shown that polyethylene glycol (PEG), a hydrophilic polymer, can quickly (within minutes of application) and effectively seal membrane breaches and reduce oxidative stress following mechanical injury [10, 14–17]. Such structural and biochemical improvement is paralleled by a significant functional restoration in both ex vivo and in vivo spinal cord injuries [14, 15, 18–21]. However, in spite of the wealth of studies demonstrating PEG's efficacy in treating acute spinal cord injury, the mechanism by which it repairs damaged membranes and reduces oxidative stress is not completely clear.

The current proposed model by which PEG reduces both primary and secondary injury following spinal cord trauma is that PEG interacts with and repairs damaged plasma membranes, which in turn indirectly reduces oxidative stress [10, 16, 17, 22]. This hypothesis is supported by strong evidence that PEG can directly interact and seal lipid bilayers [10, 16] as well as the finding that PEG is not a free radical scavenger [10]. According to this hypothesis, PEG-mediated suppression of oxidative stress is secondary to the repair of plasma membrane. Recently, several observations indicated that PEG may reduce oxidative stress through yet another pathway – by directly interacting with and protecting mitochondria [10, 23].

Mitochondria are known to play a key role in oxidative stress, as this organelle produces reactive oxygen species in the normal process of oxidative phosphorylation [24, 25]. This production of reactive oxygen species and release into the cytosol is increased following trauma and various pathological conditions where oxidative stress plays a role [26, 27]. Mitochondria are both vulnerable to and, at the same time, capable of producing free radicals. Directly improving mitochondrial function is known to reduce production of free radicals and alleviate oxidative stress [28–30]. Therefore, it is probable that direct protection of mitochondria by PEG may also contribute to overall suppression of oxidative stress by PEG following trauma. This hypothesis, however, has not been tested directly using functional and morphological analysis.

The purpose of the current study is, therefore, to examine the effect of PEG in directly improving function in purified, injured mitochondria from guinea pig central nervous system using functional analysis and morphological assessment. Mitochondria were challenged with elevated levels of H_2O_2 and/or calcium to model oxidative injury, which is commonly seen in various traumatic and chronic disease conditions [25, 27, 31–33]. While H_2O_2 is one of the most abundant oxygen free radicals, elevated calcium usually coexists and exacerbates oxidative stress [25, 27, 31–33]. Consistent with our hypothesis, we present evidence here that strongly supports the notion that PEG is indeed capable of directly reducing injury to mitochondria independent of plasma membrane repair. We further present evidence to support the hypothesis that PEG may act by directly blocking the mitochondrial permeability transition pore. This finding, along with previous studies, suggests that PEG exerts neuroprotective effects through direct interaction with mitochondria, in addition to its well-established ability to repair damaged plasma membranes.

Experimental Procedures

Animals and Mitochondria Preparation

All animals used in this study were handled in strict accordance with the NIH guide for the *Care and Use of Laboratory Animals*, and the experimental protocol was approved by the Purdue Animal Care and Usage Committee. Adult female Hartley guinea pigs, weighing 300–500 g, were anesthetized deeply with ketamine (60 mg/kg) and xylazine (10 mg/kg). They were then perfused through the heart with 500 ml of oxygenated, cold Krebs solution (in mM: NaCl 120, $NaHCO_3$ 25, $MgSO_4$ 0.5, KH_2PO_4 1.2, 2.5 $CaCl_2$, KCl 4.72 and dextrose 11) to remove blood and lower core temperature.

The guinea pigs were decapitated, the cortex was excised and minced with scissors in ice-cold homogenization buffer (in mM: 250 sucrose, 0.5 K^+ -EDTA, 10 Tris-HCL pH 7.4), and all subsequent steps were conducted at 4°C. The tissue was rinsed with homogenization buffer and processed (8 strokes) with a glass-Teflon Potter homogenizer. The resulting homogenate (50 ml) was centrifuged for 10 min at 1,300 g. The supernatant was collected and again centrifuged at 10,000 g for 10 min. The pellet was collected and suspended in 7.5% ficoll, and centrifuged in a discontinuous Ficoll gradient (7.5%, 10%) at 100,000 g for 30 min. The final pellet was resuspended in EDTA-free homogenization buffer (same as above with EDTA omitted), yielding purified non-synaptosomal mitochondria [34, 35]. The final pellet was stored on ice for use. Mitochondrial protein concentration was determined using BCA protein kit (Pierce), BSA as standard. Typically, the cortical tissue of 1 guinea pig yielded 2–3 mg/ml of isolated mitochondrial protein.

Mitochondrial Imaging

Transmission Electron Microscopy

This was kindly performed by Life Science Microscopy Facility, Purdue University. The mitochondria were pelleted in EDTA-free homogenization buffer and fixed in 2% glutaraldehyde. After rinsing, postfixation was carried out in 1% osmium tetroxide. The preparations were then dehydrated stepwise with ethanol, embedded in Epon, and sections were cut on a Porter-Blum MT-2b ultramicrotome. Staining was carried out with uranyl acetate in 50% alcohol and lead citrate. The sections were examined with FEI/Philips CM-10 bio-twin transmission electron microscope [36].

Coherent Anti-Stokes Raman Scattering and Two-Photon Excitation Fluorescence Microscopy

Coherent anti-Stokes Raman scattering (CARS) microscopy was used to image the mitochondria and examine change in size. CARS is a 4-wave mixing process in which the interaction of a pump field $E_p(\omega_p)$ and a Stokes field $E_s(\omega_s)$ with a sample generates an anti-Stokes field E_{as} at frequency $2\omega_p - \omega_s$ [37, 38]. The CARS signal is significantly enhanced when $\omega_p - \omega_s$ is tuned to a Raman band, creating the vibrational contrast. The coherent addition of CARS fields from the vibrational oscillators in the focal volume results in a large signal, permitting molecular imaging with high speed. The mitochondrial outer membrane is composed of lipids which contain large amounts of ordered CH_2 groups. The high density of CH_2 groups generates large CARS contrast without any labeling when $\omega_p - \omega_s$ is tuned to CH_2 stretching band at $2,840\text{ cm}^{-1}$. To verify CARS images of mitochondria,

we used the potentiometric probe rhodamine 123 (Rh123; Molecular Probes) [39] to label the mitochondria and image them by two-photon excitation fluorescence (TPEF). The detailed setup and procedures for CARS and TPEF imaging can be found elsewhere [40]. Briefly, the pump and Stokes laser beams were generated by 2 tightly synchronized (Sync-Lock) Ti:sapphire oscillators (Mira 900; Coherent Inc.). The pump and Stokes laser wavelengths were approximately 704 and 880 nm, respectively, with a pulse width of 2.5 ps. A Pockels' cell was placed in the laser beams to reduce the repetition rate from 78 to 7.8 MHz. The laser beams were collinearly combined and directed into a laser scanning confocal microscope (FV300/IX70; Olympus America Inc.). A 60× water immersion objective (numerical aperture 1.2) was used to focus the excitation beams into the sample. The forward-detected CARS signal was collected by an air condenser (numerical aperture 0.55) through a 600/65 nm band-pass filter, while the TPEF signal was collected from the backward detection by the same water immersion objective through a 520/40 nm band-pass filter. Both CARS and TPEF signals were detected with photomultiplier tubes.

All imaging experiments were performed at room temperature in KCl-based respiration buffer (in mM: 125 KCl, 3 KH₂PO₄, 0.5 MgCl₂, 3 succinate, 3 glutamate, 10 HEPES, 0.1% BSA pH 7.4) [34, 35]. Mitochondria were added to this buffer at a final concentration of 1 mg protein/ml immediately before each experiment. A small drop (20 ml) of mitochondrial suspension was placed in the middle of the coverslip for 5–7 min. The mitochondria were perfused slowly with respiration buffer. After 1 min of perfusion, mitochondria which had not attached to the coverslip were effectively washed out of the recording chamber. In order to confirm the image of mitochondria by CARS we added Rh123 (at a non-quenching concentration of 200 nM) to the perfusion buffer 10 min before the start of the recording, and Rh123 was present in the perfusion medium during the rest of the experiment.

The mitochondrial volume was estimated in the following manner. First, the long and short axes were measured based on the images using CARS microscopy (fig. 7). Second, a cylinder shape was assumed for the mitochondria and the volume was estimated using the following formula:

$$A = (a - b) \pi \left(\frac{b}{2}\right)^2 + \frac{4}{3} \pi \left(\frac{b}{2}\right)^3$$

where A is the mitochondrial volume, a the long axis and b the short axis (fig. 7b, inset).

As indicated in the formula, a typical mitochondria is considered to be roughly a cylinder in the middle and 2 half spheres on both ends.

The short axis (width) of the mitochondrion was measured as the full width at half maximum of CARS intensity profile across the mitochondrion (fig. 7b, inset). The long axis was measured in a similar manner.

Measurement of Oxygen Consumption

Oxygen consumption of the mitochondria was measured at 30°C in a thermostat-controlled chamber equipped with a Clark-type electrode (model 203; Instech) [41, 42]. The experiments were performed in respiration buffer [34, 35]. For calibration of the oxygen electrode, the oxygen content of the air-saturated incubation medium was taken to be 217 nmol/ml. Succinate concentration was 10 mM, and state 3 respiration initiated by the ad-

dition of 100 μM ADP. State 4 respiration followed 5 min after ADP was used up. The respiratory rates were calculated as nanomole of O₂ per minute per milligram of mitochondrial protein. The respiratory control ratio (RCR) was calculated as the ratio of the rate of state 3 respiration to the state 4 rate.

Measurement of Mitochondrial Transmembrane Potential

Mitochondrial transmembrane potential Δψ_m is estimated by the quantitation of Rh123 quenching [43]. Rh123 (at a quenching concentration of 5 μM) is concentrated in the mitochondria and is quenched at a high Δψ_m level [43]. In contrast, when Δψ_m is decreased, Rh123 is released, causing dequenching and an augmentation in Rh123 fluorescence. Therefore, in such conditions, a higher value of Rh123 is indicative of a low Δψ_m level [43]. Mitochondria (1 mg/ml) were incubated in the isolation buffer with 5 μM Rh123 for 5 min. Quenching of Rh123 fluorescence (excitation 490 nm and emission 535 nm) was measured continuously in a fluorometer [43, 44].

The Preparation of PEG Solution

Isosmotic (300 mosm) stock solutions were made for PEG at various molecular weights: PEG 1,000 (150 mM); PEG 1,500 (122 mM); PEG 2,000 (102 mM); PEG 3,400 (64 mM; pH 7.4) [45]. Such PEG stock solutions were then mixed with other isosmotic solutions to make the final PEG solutions which retain constant osmotic pressure [45].

Chemicals

ADP, K⁺-EDTA, HEPES potassium salt, KH₂PO₄, MgCl₂, succinate, mannitol, sucrose, BSA and carbonyl cyanide 4-(trifluoromethoxy) phenylhydrazone (FCCP) were purchased from Sigma-Aldrich. BCA protein assay kit and Rh123 were purchased from either Pierce or Molecular Probes.

Statistical Analysis

Data were presented as means ± SEM. One-way analysis of variance was used for data analysis. Results showing overall significance were subject to post hoc Tukey test. p < 0.05 was considered statistically significant.

Results

The Purified Nonsynaptic Brain Mitochondria

Following the procedures of purification, the health of isolated mitochondria was demonstrated through several tests. First, mitochondrial oxygen consumption was measured using a Clark electrode. The RCR value of uninjured isolated mitochondria was 5.26 ± 0.18. Furthermore, electron microscopy imaging and the combination of 2-photon confocal microscopy and CARS demonstrated that the purified mitochondria appear morphologically healthy (fig. 1). Specifically, as shown in the images from scanning electron microscopy (fig. 1d), both the inner and outer mitochondrial membranes as well as the tight cristae were clearly seen in most single mitochon-

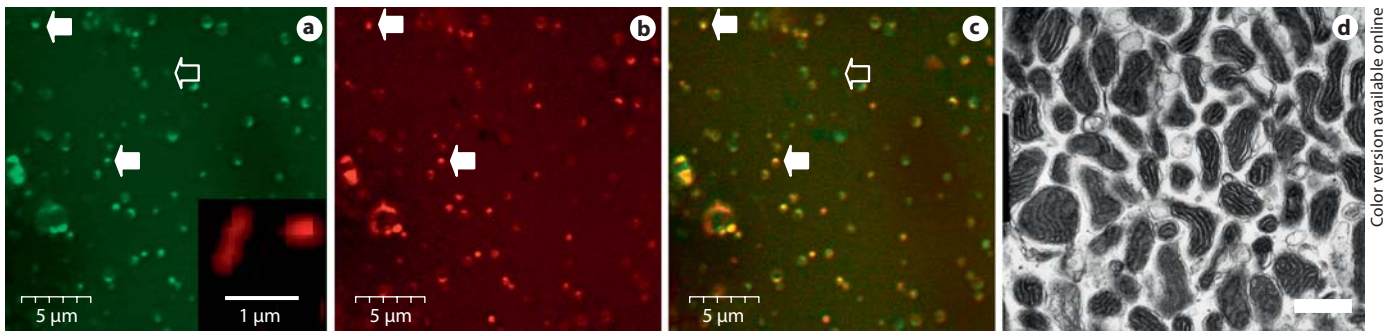


Fig. 1. Morphology of isolated mitochondria. **a–c** Nonsynaptic mitochondria isolated from guinea pig brain are imaged with CARS and TPEF microscopy. Note that most CARS images of mitochondria (solid arrows in **a**) coincide with the labeling of Rh123 (solid arrows in **b** and **c**). Only a few mitochondria imaged by CARS are lacking Rh123 (open arrow in **a** and **c**). Inset in

a shows 2 high-magnification mitochondria imaged by CARS with shapes that resemble those imaged by electron microscopy depicted in **d**. **d** Isolated mitochondria image with transmission electron microscopy. Note the isolated mitochondria are mostly rod shaped; the inner membrane is thrown into folds as cristae. Scale bar = 1 μm (**d**).

Color version available online

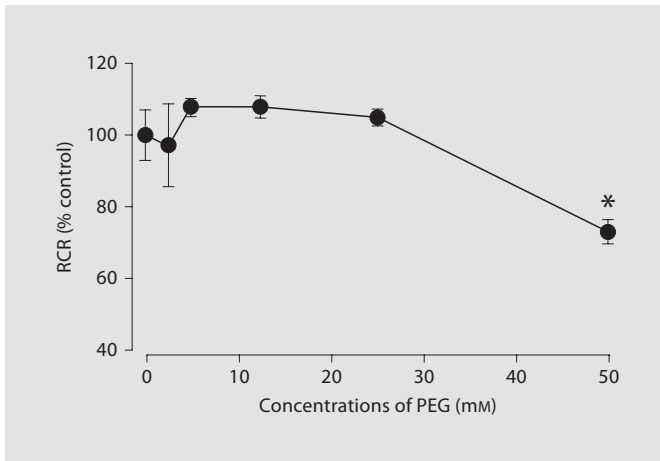


Fig. 2. RCR in isolated brain mitochondria exposed to various concentrations of PEG. Nonsynaptic mitochondria were isolated from guinea pig forebrain and incubated in the respiratory buffer at 30°C for 15 min with various concentrations of PEG (molecular weight: 2,000). Each point represents the average of 5 experiments, expressed as percent of controls. Error bars are SEM. PEG at 2.5, 5, 12.5 and 25 mM had no significant detrimental effect on RCR compared to control (no PEG). However, PEG at 50 mM significantly inhibited RCR after 15 min of incubation ($p < 0.05$). * $p < 0.05$ when compared to control.

dria with limited sign of mitochondrial deterioration. Mitochondria were also imaged by CARS microscopy. At the same time, 2-photon fluorescence microscopy was also used to observe the labeling of potentiometric probe Rh123 applied at a nonquenching concentration (200 nM)

[39]. Rh123 labeling inside the mitochondria is an indication of healthy inner mitochondrial potential and largely coincides with the images of mitochondria revealed by CARS (fig. 1a–c).

The Toxicity of PEG on the Normal Isolated Mitochondrial Respiration

The toxicity of PEG to uninjured mitochondria was first evaluated to determine the maximum safe concentration (molecular weight: 2,000). The study was conducted using oxygen consumption rate, a direct measurement of mitochondrial respirational function (fig. 2). Various concentrations of PEG (2.5, 5, 12.5, 25 and 50 mM) were incubated with uninjured nonsynaptic mitochondria. As shown in figure 2, PEG at a concentration of 50 mM significantly decreased RCR to 73.15% of the control value ($p < 0.05$). While 25 and 12.5 mM did not suppress mitochondrial respiration significantly, PEG at 12.5 mM was chosen for the remainder of the study.

Mitochondrial Dysfunction Induced by H₂O₂ and/or Ca²⁺ and Its Inhibition by PEG:

Assessment of Mitochondrial Oxygen Consumption

Nonsynaptic mitochondria were first injured by exposure to H₂O₂ at a concentration of 440 μM for 15 min. Mitochondria were then transferred to the respiratory buffer in the presence or absence of 12.5 mM PEG at 30°C for another 15 min. As shown in figure 3a, H₂O₂ caused a decrease in RCR in nonsynaptic mitochondria ($p < 0.05$ when compared to control). Interestingly, the reduction of RCR by H₂O₂ can be significantly reversed by PEG

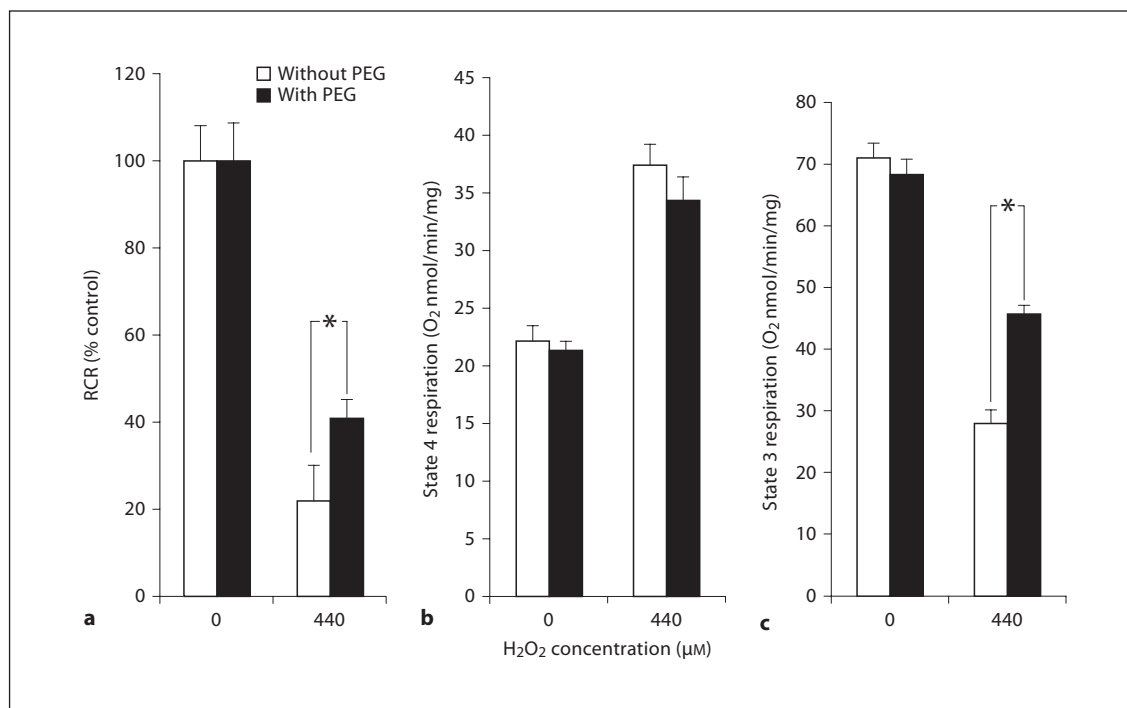


Fig. 3. Effect of H₂O₂ on the respiration in isolated mitochondria and its reversal by PEG. **a** Effect of PEG on overall RCR in the presence of H₂O₂. Nonsynaptic mitochondria were isolated from guinea pig forebrain and incubated at room temperature for 15 min in the absence or presence of H₂O₂ (440 μM). Mitochondria were then transferred to the respiratory buffer in the presence or absence of 12.5 mM PEG at 30°C for 15 min. Values were expressed as percentage of controls. Error bars are SEM. H₂O₂ produced a reduction of RCR. PEG treatment resulted in a significant increase in the RCR of mitochondria incubated in 440 μM H₂O₂ (n = 5, p < 0.05). * p < 0.05. **b** Effect of PEG on the state 4 respira-

tion of mitochondria in the presence of H₂O₂. Each bar represents the average O₂ consumption (nmol/min/mg protein) from 5 animals. Error bars are SEM. Please note that PEG treatment had no significant effect on state 4 respiration at 440 μM H₂O₂ (p > 0.05). **c** Effect of PEG on the state 3 respiration of mitochondria in the presence of H₂O₂. Each bar represents the average O₂ consumption (nmol/min/mg protein) from 5 animals. Error bars are SEM. PEG treatment resulted in a significant increase in the state 3 respiration of mitochondria in the presence of 440 μM H₂O₂ (p < 0.05). * p < 0.05.

(12.5 mM; fig. 3a). Specifically, PEG incubation resulted in a significant increase in RCR from 22% (H₂O₂ only) to 41% (H₂O₂ plus PEG) of control. PEG-mediated mitochondrial functional recovery was mainly due to the improvement of oxygen consumption in state 3 (from 27.86 to 45.64 nmol/ml/mg, p < 0.05) and not in the state 4 (fig. 3b, c).

In addition to H₂O₂, we have also shown that exposure to elevated Ca²⁺ (50 μM) inflicted a reduction of RCR of the nonsynaptic mitochondria (fig. 4; p < 0.05 when compared to control). However, PEG treatment resulted in a significant increase in the RCR of mitochondria challenged with 50 μM Ca²⁺ (from 61.98 to 89.26% of control value, p < 0.05).

Finally, when nonsynaptic mitochondria were exposed to H₂O₂ (88 μM) and Ca²⁺ (25 M), a further sig-

nificant reduction of RCR was observed compared to control (fig. 5; p < 0.01). Such reduction of RCR is significantly more severe compared to the decrease in RCR produced by either factor alone (p < 0.05). In such a condition where both Ca²⁺ and H₂O₂ were present, 12.5 mM PEG treatment increased the RCR in mitochondria from 42.33 to 71.96% of the control (fig. 5; p < 0.05). Cyclosporine A at 200 μM further improved the RCR compared to control (p < 0.01) or in the presence of PEG (p < 0.05).

Effects of PEG on the H₂O₂-Induced Changes in Mitochondrial Membrane Potential

Mitochondrial membrane potential was monitored for about 500 s, and Rh123 (at a quenching concentration of 5 μM) was used to denote the status of mitochondrial

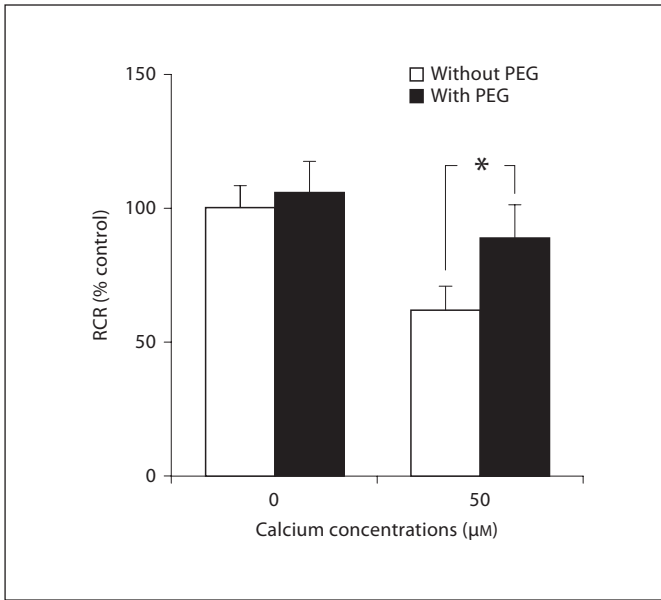


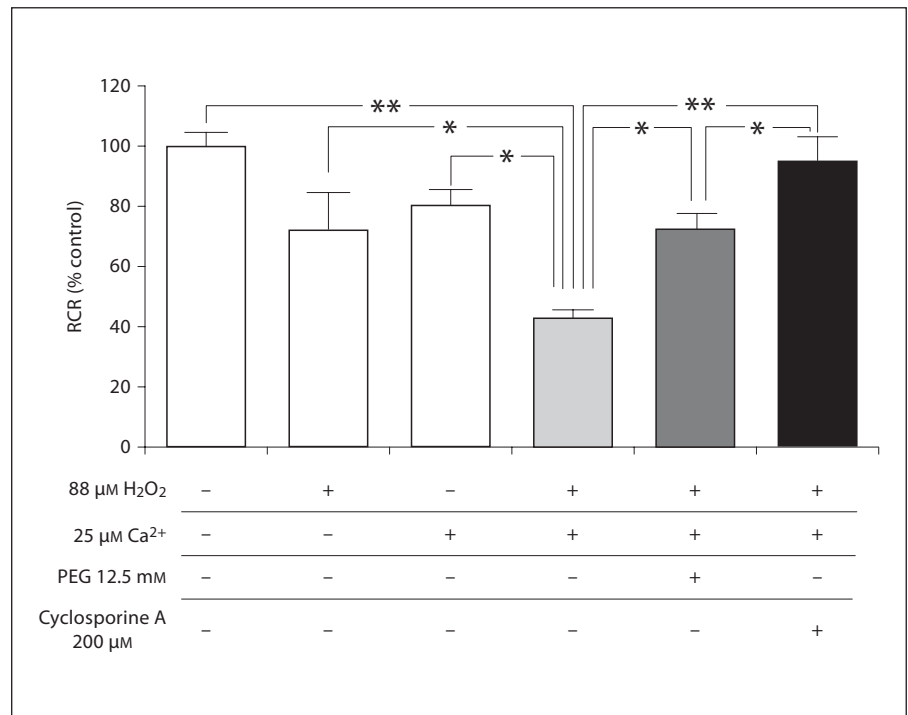
Fig. 4. Effect of PEG on the RCR of isolated brain mitochondria exposed to Ca^{2+} . Nonsynaptic mitochondria were isolated from guinea pig forebrain and preincubated in the respiratory buffer with or without 12.5 mM PEG for 15 min at 30°C. Ca^{2+} (50 μM) was added immediately before succinate was added. Values were expressed as percent of controls. Error bars are SEM. Preincubation with PEG resulted in a significant increase in the RCR of mitochondria challenged with 50 μM Ca^{2+} ($n = 5$, $p < 0.05$). * $p < 0.05$.

membrane potential. As shown in figure 6, at 100 s from the beginning of the observation, 440 μM H_2O_2 was added to the solution to induce a decrease (or depolarization) in mitochondrial membrane potential, denoted by an increase in Rh123 absorbance. At 150 s from the beginning of the observation or 50 s following the addition of H_2O_2 (point A in fig. 6), either PBS (control) or 12.5 mM PEG (treated group) was applied to the solution bathing injured mitochondria. At approximately 430 s from the beginning or 330 s following H_2O_2 application (point B of fig. 6), data were taken to compare the membrane potential in the H_2O_2 or the H_2O_2 plus PEG group. It is evident that the decrease in Rh123 fluorescence (or the recovery of mitochondrial membrane potential) was significantly greater in the PEG-treated group. Specifically, PEG significantly decreased the depolarization to 36% (H_2O_2 and PEG treated) compared to 75% (H_2O_2 alone) at the time point of examination (point B in fig. 6; $n = 6$, $p < 0.01$).

Effects of PEG on the Morphology of Isolated Mitochondria Injured by Ca^{2+} Using CARS Microscopy

The morphology of isolated mitochondria was observed by CARS microscopy. The advantage of such imaging is that no exogenous labeling molecules are needed,

Fig. 5. Effect of PEG on the RCR of mitochondria exposed to H_2O_2 and Ca^{2+} . Nonsynaptic mitochondria were isolated from guinea pig forebrain and incubated at room temperature for 15 min and then transferred to the respiratory buffer in the presence or absence of 12.5 mM PEG. Either H_2O_2 (88 μM) or calcium (25 μM) or both H_2O_2 and calcium was added to the solution. Specifically, H_2O_2 was included in the incubation media for 15 min before transferring to respiratory buffer. Calcium was added immediately before the addition of succinate. Values were expressed as percent of controls. Error bars are SEM. Note that 88 μM H_2O_2 and 25 μM Ca^{2+} significantly inhibited the RCR of mitochondria than either H_2O_2 or Ca^{2+} alone ($p < 0.05$). This inhibition was significantly reduced when PEG was present ($p < 0.05$) or in the presence of cyclosporine A ($p < 0.05$). $n = 5-8$ in all groups. * $p < 0.05$; ** $p < 0.01$.



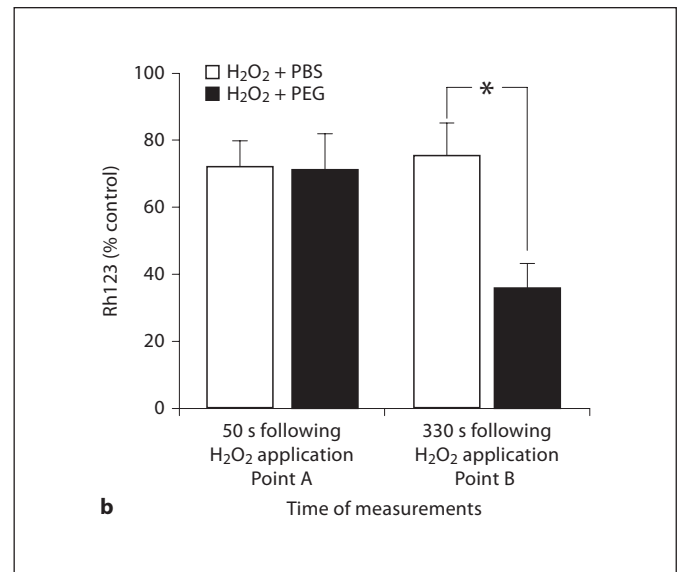
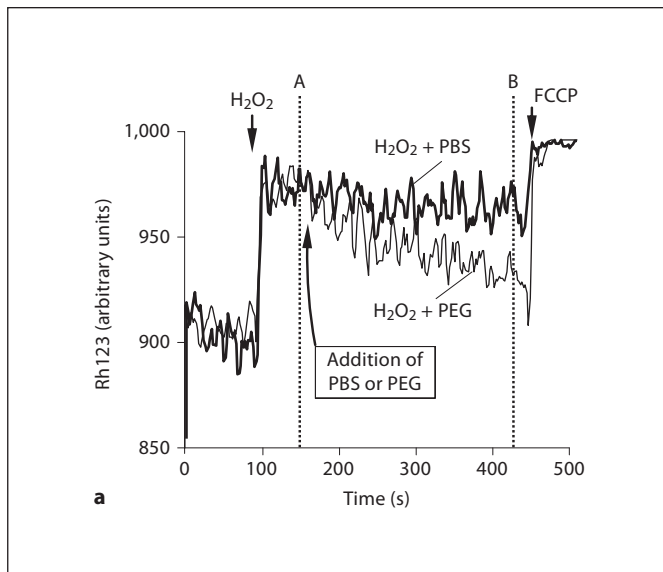


Fig. 6. Effect of PEG on the mitochondrial membrane potential in the presence of H_2O_2 . **a** Nonsynaptic mitochondria were isolated from guinea pig forebrain. Mitochondrial transmembrane potential was monitored using Rh123. H_2O_2 at a concentration of 0.015% was applied to induce the mitochondrial membrane potential change (depolarization), followed by 12.5 mM of PEG or PBS. Finally, FCCP (2 μM) was employed to collapse the membrane potential. Shown here is a representative trace displaying the mitochondrial membrane potential depolarization in the response to H_2O_2 . However, H_2O_2 -mediated mitochondrial mem-

brane depolarization was significantly attenuated with the addition of PEG, but not PBS (control). Note the significant reduction of Rh123 fluorescence following the addition of PEG, but not the addition of PBS (control). **b** Quantification of Rh123 fluorescence in various conditions examined at the time points denoted in **a**. Values are expressed as the percent of control, calculated as baseline subtracted from FCCP-collapsed membrane potential. Error bars are SEM. Note that 12.5 mM PEG significantly decreased Rh123 fluorescence which was induced by H_2O_2 . $n = 6$ in all groups. * $p < 0.01$.

so the size of the mitochondria can be observed in their most native and undisturbed condition. As shown in figure 7a, the typical single thin mitochondria were clearly seen in the control group using CARS microscopy. Following incubation in 100 μM Ca^{2+} for 15 min, mitochondrial swelling was evident as the size of the mitochondria were significantly increased (fig. 7b). However, mitochondrial swelling was reduced in the PEG-treated samples (fig. 7c). When the mitochondrial volume was estimated, it became evident that Ca^{2+} induced a significant increase in mitochondrial volume, and PEG treatment almost completely reversed swelling. Specifically, the average volume of uninjured mitochondria was $0.68 \pm 0.02 \mu m^3$ ($n = 226$). This value was increased to $1.02 \pm 0.03 \mu m^3$ in the presence of Ca^{2+} ($n = 143$, $p < 0.05$ compared to control). However, PEG significantly decreased the mitochondrial volume induced by Ca^{2+} to $0.73 \pm 0.02 \mu m^3$ ($n = 143$, $p < 0.05$ when compared to Ca^{2+} only, $p > 0.05$ when compared to control; fig. 7).

PEG-Mediated Mitochondrial Protection Is Dependent on the Size of PEG

In order to explore whether PEG-mediated mitochondrial protection is dependent on the size of PEG molecules, PEG at different molecular weights (1, 1.5, 2 and 3.4 kDa) were examined for their effect on the alleviation of mitochondrial functional deficits inflicted by H_2O_2 . As shown in figure 8, 440 μM H_2O_2 reduced mitochondrial RCR. However, PEG at 1.5 kDa significantly improved the RCR of mitochondria in the presence of H_2O_2 from 22.79 to 49.58% of the control ($n = 5$, $p < 0.05$). Similarly, but to a lesser degree, PEG at 2 kDa also significantly improved mitochondrial RCR to 41.23% of control ($n = 5$, $p < 0.05$). In contrast, PEG at either higher or lower molecular weights (1 and 3.4 kDa) failed to exert a significant improvement on the oxygen consumption of mitochondria in the presence of H_2O_2 .

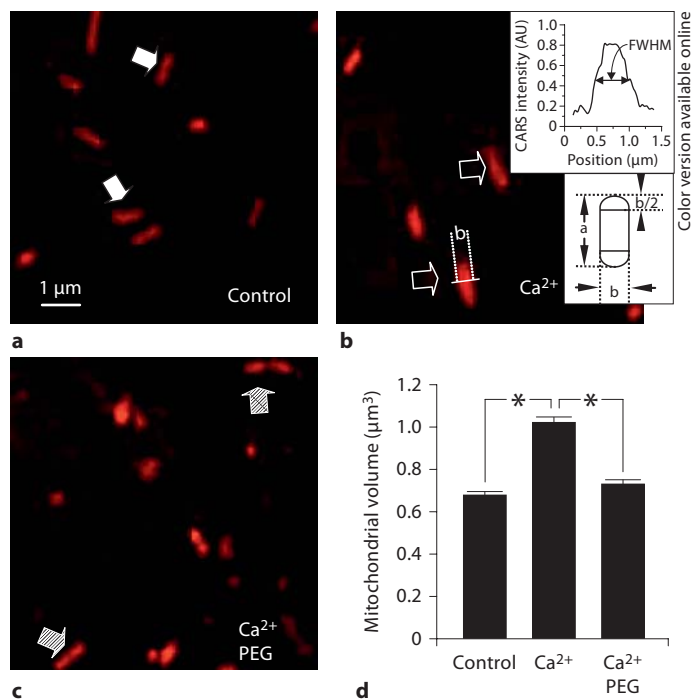


Fig. 7. Effect of PEG on the morphology of isolated mitochondria induced by Ca^{2+} using CARS. Nonsynaptic mitochondria were isolated from guinea pig forebrain and incubated at room temperature in the respiratory buffer for 15 min in control (no Ca^{2+} , no PEG; **a**), in the presence of $100 \mu\text{M}$ Ca^{2+} (**b**) or in the presence of $100 \mu\text{M}$ Ca^{2+} and 12.5 mM PEG (**c**). Please note that elevated calcium induced a significant swelling of mitochondria, and PEG significantly inhibited the Ca^{2+} -induced mitochondrial swelling. **d** Quantification of the volume of mitochondria in 3 different conditions. The solid arrows indicate the mitochondria in control (uninjured), the open arrows denote the mitochondria exposed to $100 \mu\text{M}$ calcium (injured) and the hatched arrows indicate the mitochondria exposed to $100 \mu\text{M}$ calcium and 12.5 mM PEG (injured and treated). Note the significant increase in mitochondrial volume in the Ca^{2+} -treated group and the reduction of mitochondrial volume as a result of PEG application. * $p < 0.05$. Also, note the diagrammatic description of the procedures of estimating the volume of mitochondria in **b** (lower inset). The short axis (width) of mitochondrion was measured as the full width at half maximum (FWHM) of CARS intensity profile across mitochondrion (**b**, upper inset). The long axis was measured in a similar manner.

Discussion

Previous Studies Regarding PEG-Mediated Improvement of Mitochondrial Function

In our previous studies using both in vivo and ex vivo traumatic spinal cord injury, we have shown that PEG can both effectively repair plasma membrane, a primary

injury, and significantly reduce oxidative stress, a secondary injury [10, 14–18, 22]. We have also shown that PEG is neither a free radical scavenger, nor an effective inhibitor of key enzymes that are responsible for O_2^- generation [10]. Therefore, it was concluded that PEG inhibits O_2^- and consequently lipid peroxidation mainly through the restoration of plasma membrane integrity [10].

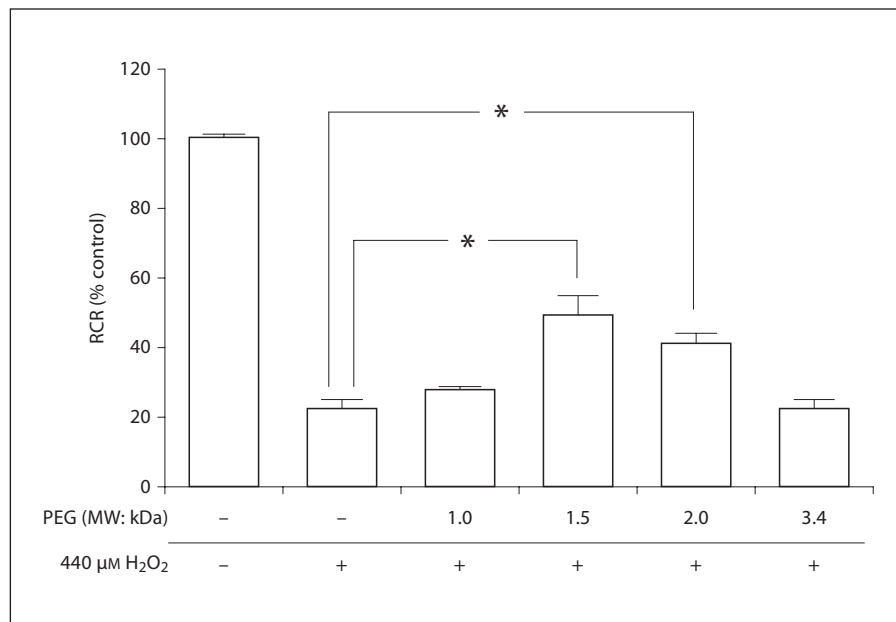
Mitochondria are a rich source of free radicals in many pathological conditions, including trauma [24, 25, 27]. Impairment of mitochondria results in increased production of free radicals [7, 27]. Hence, it has been long suspected that PEG may reduce oxidative stress by not only repairing plasma membrane, but also directly interacting with mitochondria to reduce overall oxidative stress [17]. There are several lines of evidence to support the hypothesis that PEG can directly interact with mitochondria and improve their function following mechanical spinal cord injury. First, PEG has been shown to significantly improve mitochondrial function in isolated spinal cord tissues and in live animals following spinal cord injury [17]. Second, it has been shown that PEG is capable of entering mechanically injured cells, likely through disrupted membranes, which places PEG in a position to directly interact with intracellular organelles such as mitochondria [17]. Furthermore, PEG attenuates calcium-induced functional compromise of spinal cord synaptosomal mitochondria [17]. However, these circumstantial findings are still inconclusive. One of the problems is that it is still possible that PEG-mediated improvement of mitochondria is due entirely to the indirect result of repairing the injured membrane. Therefore, the ability of PEG to directly improve purified mitochondria in a cell-free system, coupled with critical functional examination must be demonstrated to rigorously test the possibility of direct protection of mitochondria by PEG.

The Direct Protection of Mitochondria by PEG:

The Dual Action of PEG in Neuronal Protection

Compared to previous studies regarding direct PEG-mediated mitochondria protection, the current study combined 2 new critical methodologies: preparation of isolated nonsynaptosomal mitochondria and the oxygen consumption test. In such experimental conditions, PEG was in direct contact with mitochondria without the intermediate structure of plasma membrane or synaptosomal membrane. We have found that PEG at a nontoxic concentration of 12.5 mM can significantly preserve the mitochondrial oxygen consumption rate in the events

Fig. 8. PEG-mediated amelioration of the mitochondrial respiratory functional reduction due to H₂O₂ is dependent on the molecular weight of PEG. Nonsynaptic mitochondria were isolated from guinea pig forebrain and incubated in respiratory buffer at 30°C for 15 min in the presence of 440 μM H₂O₂. Mitochondria were then transferred to the respiratory buffer in the presence or absence of PEG with different molecular weights. Values were expressed as percentage of controls. Error bars are SEM. Note the biphasic effects of PEG in improving mitochondrial respiratory function. Specifically, incubation with PEG at 1.5 and 2 kDa can significantly inhibit the reduction of RCR induced by H₂O₂ (n = 5, p < 0.05). However, PEG at 1 and 3.4 kDa did not significantly inhibit H₂O₂-induced reduction of RCR (p > 0.05). * p < 0.05.



of injury caused by high calcium and H₂O₂. These findings strongly suggest that PEG does possess the ability to directly interact with mitochondria and offer protection in the event of injury. In addition to critical functional tests, we have also obtained direct morphological evidence of significant improvement of mitochondria upon PEG exposure. Specifically, we have found that PEG can effectively reduce swelling of injured mitochondria through direct imaging by CARS microscopy. Using CARS, we were able for the first time to observe live mitochondrial images without any fluorescent dye. Based on our knowledge, this is the first time for the volume of live mitochondria to be estimated without any labeling. Recently, we have shown that PEG, at a concentration that is similar to that used in the current study (10 mM), can reduce the release of cytochrome c, a proapoptotic cell death factor from isolated mitochondria, which further indicates a direct protection of mitochondria by PEG [46].

In summary, based on these critical functional and structural analyses, we have now concluded that PEG is indeed capable of directly interacting with mitochondria to preserve structure and restore function in the event of injury. Based on this finding, coupled with evidence that PEG enters the cytosol following mechanical trauma, we postulate that there are likely at least 2 avenues of PEG-mediated cytoprotection in mechanically injured spinal cord: repair of plasma membrane and protection of mi-

tochondria. Consequently, both plasma membrane repair and mitochondrial protection work synergistically to curtail oxidative stress, a hallmark of secondary injury, and enhance overall recovery.

The Mechanisms of Direct Mitochondrial Protection: Physical Inhibition of MPTP?

Despite the strong evidence that PEG can directly repair damaged mitochondria, the mechanism of such action is not clear. However, we have obtained some preliminary evidence suggesting that such protection may in part be due to physical characters of PEG. Specifically, we have found that the PEG-mediated mitochondrial protection is dependent on the size of PEG molecules. While PEG at 1.5 and 2.0 kDa are effective in protecting mitochondria under the stress of high calcium and high H₂O₂, PEG molecules that are either smaller (1.0 kDa) or larger (3.5 kDa) failed to do so.

It has been reported that formation of the mitochondrial permeability transitional pore (MPTP) is a critical pathological phenomenon in injured mitochondria [47, 48]. Blocking the MPTP restores function and suppresses oxidative stress [49–51]. Therefore, we postulate that PEG may protect mitochondria by physically blocking the MPTP. Indeed, the dependency of molecular weights of PEG-mediated mitochondrial protection is consistent with the notion of a physical blockage of MPTP by PEG. Furthermore, the size exclusion properties of the MPTP

have been reported before using both PEG and mitochondria from liver and heart [45, 52, 53]. Consistent with the hypothesis that PEG blocks MPTP, we have recently demonstrated that PEG reduces the release of cytochrome *c*, a factor that can be released from mitochondria through MPTP [46].

One interesting phenomenon regarding these studies is that the ranges of sizes of PEG that can effectively block MPTP is not in agreement among the aforementioned studies. While some of them are consistent with ours regarding the effective molecular weights of PEG in blocking MPTP [52], others are not [53]. One possible explanation for this discrepancy is that the sizes of MPTP may vary depending on the agent that induces its formation and the sources of the mitochondria, as suggested by Pfeiffer et al. [45]. For example, we used H₂O₂ to induce the formation of MPTP of the mitochondria isolated from guinea pig brain, while others used a different method, such as peptides and calcium, to induce MPTP from the mitochondria isolated from liver or heart [45, 52, 53].

Based on our findings, we postulate that the blockage of MPTP by PEG at 1.5 kDa, and to a lesser degree the PEG at 2.0 kDa, represents a relatively tight fit of PEG molecules with the MPTP, or a 'snug' plug of PEG to the MPTP. We also reason that PEG at 1.0 kDa was unable to block MPTP because these molecules are smaller than the opening of MPTP. Therefore, they will enter mitochondria through the MPTP without being 'stuck', and consequently will not block the MPTP. The reason why the 3.4-kDa PEG cannot block MPTP is probably due to the fact that it is significantly larger than MPTP. Therefore, it cannot effectively match the opening of the MPTP and consequently failed to block MPTP. However, further morphological evidence is needed to confirm such hypothesis.

The fact that PEG-mediated mitochondrial protection is only possible within a certain molecular range is interesting, considering PEG at a wide molecular range (0.4–3.5 kDa) has been shown to be effective in repairing plasma membranes and enhance functional recovery [14, 15, 18]. This discrepancy itself is probably an indication that the mechanisms of these 2 types of PEG action, PEG-mediated plasma membrane repair and direct mitochondrial protection, are different. Specifically, the proposed key factor of PEG-mediated plasma membrane repair is its hydrophilic nature [14, 15, 18]. Although not well established, it is commonly believed that PEG attracts the water positioned within the membrane breaches and encourages the lipid bilayer to fuse together and conse-

quently eliminate the gap and seal the membrane disruption. It is interesting to point out that while the overall size changed significantly from 0.4 to 3.5 kDa, PEG retains strong hydrophilic nature in this molecular range [54], which is consistent with the finding that PEG retains its ability to seal plasma membrane. In contrast, we propose that the critical factor in PEG-mediated direct mitochondrial protection is molecular weight, which determines its size and thus the ability to physically block the MPTP.

For PEG to effectively repair mitochondrial damage, it needs to reach a certain intracellular concentration. For example, for 1.5-kDa PEG, we found a concentration of 12.5 mM to be effective in inhibiting mitochondrial swelling in vitro (current study). Since this is only 1.9% of the concentration of PEG (about 667 mM) applied to spinal cord in vivo [18], we believe that this concentration is achievable in vivo. Further experiments will be needed to determine if PEG could reach an effective concentration when administered in vivo, and then it does not reach a toxic concentration of 50 mM.

The Advantages of PEG as a Neuroprotectant for Trauma and Other Neuronal Disorders

In the past few years, PEG has been shown not only to effectively repair damaged neuronal plasma membranes in spinal cord injury, but also similar deficits in traumatic brain injuries [10, 14, 16, 18, 55]. Based on the current study, PEG is also capable of directly alleviating functional and anatomical deficits in mitochondria and improving overall neurological function. Since mitochondrial injury has recently emerged as a key factor in many degenerative diseases, including Parkinson's and Alzheimer's diseases [33, 56–58], it is possible that the PEG may also be effective at treating such diseases. The dual action of PEG and its relatively low toxicity make this a very attractive potential treatment for acute as well as chronic neurodegenerative diseases.

Acknowledgements

This study was supported by grants from NIH-NINDS, NSF and the State of Indiana. We thank Phyllis Zickmund, Debbie Bohnert and Drs. Jian Luo, Richard Borgens and J. Paul Robinson for their invaluable assistance.

References

- 1 Meiri H, Spira ME, Parnas I: Membrane conductance and action potential of a regenerating axon tip. *Science* 1981;211:709–712.
- 2 Yawo H, Kuno M: How a nerve fiber repairs its cut end: involvement of phospholipase A2. *Science* 1983;222:1351–1352.
- 3 Xie X, Barrett JN: Membrane resealing in cultured rat septal neurons after neurite transection: evidence for enhancement by Ca²⁺-triggered protease activity and cytoskeletal disassembly. *J Neurosci* 1991;11:3257–3267.
- 4 Shi R, Asano T, Vining NC, Blight AR: Control of membrane sealing in injured mammalian spinal cord axons. *J Neurophysiol* 2000;84:1763–1769.
- 5 Shi R, Pryor JD: Pathological changes of isolated spinal cord axons in response to mechanical stretch. *Neuroscience* 2002;110:765–777.
- 6 Shi R: The dynamics of axolemmal disruption in guinea pig spinal cord following compression. *J Neurocytol* 2004;33:203–211.
- 7 Hall ED: Free radicals and CNS injury. *Crit Care Clin* 1989;5:793–805.
- 8 Povlishock JT, Kontos HA: The role of oxygen radicals in the pathobiology of traumatic brain injury. *Hum Cell* 1992;5:345–353.
- 9 Hall ED: Lipid peroxidation. *Adv Neurol* 1996;71:247–257, discussion 57–58.
- 10 Luo J, Borgens RB, Shi R: Polyethylene glycol immediately repairs neuronal membranes and inhibits free radical production after acute spinal cord injury. *J Neurochem* 2002;83:471–480.
- 11 Luo J, Li N, Paul Robinson J, Shi R: Detection of reactive oxygen species by flow cytometry after spinal cord injury. *J Neurosci Methods* 2002;120:105.
- 12 Tator CH, Fehlings MG: Review of the secondary injury theory of acute spinal cord trauma with emphasis on vascular mechanisms. *J Neurosurg* 1991;75:15–26.
- 13 Povlishock JT: Pathophysiology of neural injury: therapeutic opportunities and challenges. *Clin Neurosurg* 2000;46:113–126.
- 14 Shi R, Borgens RB: Acute repair of crushed guinea pig spinal cord by polyethylene glycol. *J Neurophysiol* 1999;81:2406–2414.
- 15 Shi R, Borgens RB, Blight AR: Functional reconnection of severed mammalian spinal cord axons with polyethylene glycol. *J Neurotrauma* 1999;16:727–738.
- 16 Shi R, Borgens RB: Anatomical repair of nerve membranes in crushed mammalian spinal cord with polyethylene glycol. *J Neurocytol* 2000;29:633–643.
- 17 Luo J, Borgens R, Shi R: Polyethylene glycol improves function and reduces oxidative stress in synaptosomal preparations following spinal cord injury. *J Neurotrauma* 2004;21:994–1007.
- 18 Borgens RB, Shi R: Immediate recovery from spinal cord injury through molecular repair of nerve membranes with polyethylene glycol. *FASEB J* 2000;14:27–35.
- 19 Borgens RB, Bohnert D: Rapid recovery from spinal cord injury following subcutaneously administered polyethylene glycol. *J Neurosci Res* 2001;66:1179–1186.
- 20 Borgens RB, Shi R, Bohnert D: Behavioral recovery from spinal cord injury following delayed application of polyethylene glycol. *J Exp Biol* 2002;205:1–12.
- 21 Donaldson J, Shi R, Borgens R: Polyethylene glycol rapidly restores physiological functions in damaged sciatic nerves of guinea pigs. *Neurosurgery* 2002;50:147–156.
- 22 Luo J, Shi R: Diffusive oxidative stress following acute spinal cord injury in guinea pigs and its inhibition by polyethylene glycol. *Neurosci Lett* 2004;359:167–170.
- 23 Chen H, Shi R: Polyethylene glycol improves function of isolated brain mitochondria: implication in central nervous system trauma. *J Neurotrauma* 2004;21:1303.
- 24 Cadenas E, Davies KJ: Mitochondrial free radical generation, oxidative stress, and aging. *Free Radic Biol Med* 2000;29:222–230.
- 25 Lenaz G, Bovina C, D'Aurelio M, Fato R, Formiggini G, Genova ML, Giuliano G, Pich MM, Paolucci U, Castelli GP, Ventura B: Role of mitochondria in oxidative stress and aging. *Ann NY Acad Sci* 2002;959:199–213.
- 26 Hall ED, Braughler JM: Free radicals in CNS injury. *Res Publ Assoc Res Nerv Ment Dis* 1993;71:81–105.
- 27 Halliwell B, Gutteridge JMC: *Free Radicals in Biology and Medicine*. Oxford, Oxford University Press, 1999.
- 28 Brustovetsky N, Dubinsky JM: Limitations of cyclosporin A inhibition of the permeability transition in CNS mitochondria. *J Neurosci* 2000;20:8229–8237.
- 29 Morin D, Hauet T, Spedding M, Tillement J: Mitochondria as target for antiischemic drugs. *Adv Drug Deliv Rev* 2001;49:151–174.
- 30 Anders MW, Robotham JL, Sheu SS: Mitochondria: new drug targets for oxidative stress-induced diseases. *Expert Opin Drug Metab Toxicol* 2006;2:71–79.
- 31 Sims NR, Anderson MF: Mitochondrial contributions to tissue damage in stroke. *Neurochem Int* 2002;40:511–526.
- 32 Wingrave JM, Schaecher KE, Sribnick EA, Wilford GG, Ray SK, Hazen-Martin DJ, Hogan EL, Banik NL: Early induction of secondary injury factors causing activation of calpain and mitochondria-mediated neuronal apoptosis following spinal cord injury in rats. *J Neurosci Res* 2003;73:95–104.
- 33 Ohta S, Ohsawa I: Dysfunction of mitochondria and oxidative stress in the pathogenesis of Alzheimer's disease: on defects in the cytochrome c oxidase complex and aldehyde detoxification. *J Alzheimers Dis* 2006;9:155–166.
- 34 Lai JC, Clark JB: Preparation of synaptic and nonsynaptic mitochondria from mammalian brain. *Methods Enzymol* 1979;55:51–60.
- 35 Jin Y, McEwen ML, Nottingham SA, Maragos WF, Dragicevic NB, Sullivan PG, Springer JE: The mitochondrial uncoupling agent 2,4-dinitrophenol improves mitochondrial function, attenuates oxidative damage, and increases white matter sparing in the contused spinal cord. *J Neurotrauma* 2004;21:1396–1404.
- 36 Tonshin AA, Saprunova VB, Solodovnikova IM, Bakeeva LE, Yaguzhinsky LS: Functional activity and ultrastructure of mitochondria isolated from myocardial apoptotic tissue. *Biochemistry (Mosc)* 2003;68:875–881.
- 37 Maker PD, Terhune RW: Study of optical effects due to an induced polarization third order in the electric field strength. *Phys Rev* 1965;137:A801–A818.
- 38 Shen YR: *The Principles of Nonlinear Optics*. New York, John Wiley and Sons Inc., 1984.
- 39 Vergun O, Votyakova TV, Reynolds IJ: Spontaneous changes in mitochondrial membrane potential in single isolated brain mitochondria. *Biophys J* 2003;85:3358–3366.
- 40 Wang H, Fu Y, Zickmund P, Shi R, Cheng JX: Coherent anti-stokes Raman scattering imaging of axonal myelin in live spinal tissues. *Biophys J* 2005;89:581–591.
- 41 Li N, Ragheb K, Lawler G, Sturgis J, Rajwa B, Melendez JA, Robinson JP: Mitochondrial complex I inhibitor rotenone induces apoptosis through enhancing mitochondrial reactive oxygen species production. *J Biol Chem* 2003;278:8516–8525.
- 42 Luo J, Robinson JP, Shi R: Acrolein-induced cell death in PC12 cells: role of mitochondria-mediated oxidative stress. *Neurochem Int* 2005;47:449–457.
- 43 Zamzami N, Maise C, Metivier D, Kroemer G: Measurement of membrane permeability and permeability transition of mitochondria. *Methods Cell Biol* 2001;65:147–158.
- 44 Emaus RK, Grunwald R, Lemasters JJ: Rhodamine 123 as a probe of transmembrane potential in isolated rat-liver mitochondria: spectral and metabolic properties. *Biochim Biophys Acta* 1986;850:436–448.
- 45 Pfeiffer DR, Gudz TI, Novgorodov SA, Erdahl WL: The peptide mastoparan is a potent facilitator of the mitochondrial permeability transition. *J Biol Chem* 1995;270:4923–4932.

- 46 Luo J, Shi R: Polyethylene glycol inhibits apoptotic cell death following traumatic spinal cord injury. *Brain Res* 2007;1155:10–16.
- 47 Crompton M: The mitochondrial permeability transition pore and its role in cell death. *Biochem J* 1999;341:233–249.
- 48 Zamzami N, Kroemer G: The mitochondrion in apoptosis: how Pandora's box opens. *Nat Rev Mol Cell Biol* 2001;2:67–71.
- 49 Friberg H, Ferrand-Drake M, Bengtsson F, Halestrap AP, Wieloch T: Cyclosporin A, but not FK 506, protects mitochondria and neurons against hypoglycemic damage and implicates the mitochondrial permeability transition in cell death. *J Neurosci* 1998;18:5151–5159.
- 50 Gores GJ, Miyoshi H, Botla R, Aguilar HI, Bronk SF: Induction of the mitochondrial permeability transition as a mechanism of liver injury during cholestasis: a potential role for mitochondrial proteases. *Biochim Biophys Acta* 1998;1366:167–175.
- 51 Kowaltowski AJ, Castilho RF, Vercesi AE: Mitochondrial permeability transition and oxidative stress. *FEBS Lett* 2001;495:12–15.
- 52 Haworth RA, Hunter DR: The Ca²⁺-induced membrane transition in mitochondria. II. Nature of the Ca²⁺ trigger site. *Arch Biochem Biophys* 1979;195:460–467.
- 53 Le Quoc K, Le Quoc D: Involvement of the ADP/ATP carrier in calcium-induced perturbations of the mitochondrial inner membrane permeability: importance of the orientation of the nucleotide binding site. *Arch Biochem Biophys* 1988;265:249–257.
- 54 Harris JM, Zalipsky S: *Poly(ethylene Glycol) Chemistry and Biological Applications*. Washington DC, American Chemistry Society, 1997.
- 55 Koob AO, Duerstock BS, Babbs CF, Sun Y, Borgens RB: Intravenous polyethylene glycol inhibits the loss of cerebral cells after brain injury. *J Neurotrauma* 2005;22:1092–1111.
- 56 Kosel S, Hofhaus G, Maassen A, Vieregge P, Graeber MB: Role of mitochondria in Parkinson disease. *Biol Chem* 1999;380:865–870.
- 57 Panov A, Dikalov S, Shalbuyeva N, Taylor G, Sherer T, Greenamyre JT: Rotenone model of Parkinson disease: multiple brain mitochondria dysfunctions after short term systemic rotenone intoxication. *J Biol Chem* 2005;280:42026–42035.
- 58 Wieloch T: Mitochondrial involvement in acute neurodegeneration. *IUBMB Life* 2001;52:247–254.